0013-7227/05/$15.00/0
Printed in U.S.A.

Endocrinology 146(3):1138–1144

doi: 10.1210/en.2004-1115

Increased Neurogenesis in Dentate Gyrus of Long-Lived Ames Dwarf Mice

Liou Y. Sun, M. Steven Evans, Jenny Hsieh, Jacob Panici, and Andrzej Bartke

Geriatrics Research (L.Y.S., J.P., A.B.), Department of Internal Medicine (L.Y.S., J.P., A.B.), Department of Physiology (L.Y.S., A.B.), and Department of Neurology (S.E.), Southern Illinois University School of Medicine, Springfield, Illinois 62794; and Laboratory of Genetics (J.H.), The Salk Institute, La Jolla, California 92037

Neurogenesis occurs throughout adult life in the dentate gyrus of mammalian hippocampus and has been suggested to play an important role in cognitive function. Multiple trophic factors including IGF-I have been demonstrated to regulate hippocampal neurogenesis. Ames dwarf mice live considerably longer than normal animals and maintain physiological function at youthful levels, including cognitive function, despite a deficiency of circulating GH and IGF-I. Here we show an increase in numbers of newly generated cells [bromodeoxyuridine (BrdU) positive] and newborn neurons (neuronal nuclear antigen and BrdU positive) in the dentate gyrus of adult dwarf mice compared with normal mice using BrdU labeling. Despite the profound suppression of hippocampal GH expression, hippocampal IGF-I protein levels are up-regulated and the corresponding mRNAs are as high in Ames dwarf as in normal mice. Our results suggest that local/hippocampal IGF-I expression may have induced the increase in hippocampal neurogenesis, and increased neurogenesis might contribute to the maintenance of youthful levels of cognitive function during aging in these long-lived animals. (*Endocrinology* 146: 1138–1144, 2005)

IT IS WELL documented that neurogenesis persists in specific regions of adult mammalian brains (1). In rodent, monkey, and human, newborn neurons are continuously generated throughout adulthood in the dentate gyrus (DG) of the hippocampus (2–4). In the subgranular cell layer of the DG, hippocampal progenitors proliferate and migrate a short distance into the granule cell layer, where they differentiate into hippocampal granule cells (5). Although the functional significance of this ongoing neurogenesis in the DG is not fully defined, evidence has been provided that newly produced neurons play an important role in hippocampal cognitive function (6, 7). In addition, increased neurogenesis can reverse age-associated memory impairment, suggesting that a slowing of neuronal stem cell proliferation with age might play a role in age-associated memory impairment (8, 9).

The neural progenitor cells can respond to environmental demands, including brain injury, increased mental and physical activity, and dietary manipulations, by increasing their proliferation or survival (10–14). The signals that influence neural progenitor cell fate are being identified and include various growth factors and cytokines (1). Among the multiple growth factors that may regulate neurogenesis, IGF-I is of particular interest because of its role in growth regulation throughout the lifespan (15, 16). Overexpression of IGF-I, both peripherally and centrally, in transgenic mice results in an increase in brain size and myelin content (17, 18), whereas transgenic mice with ectopic brain expression of IGF-binding protein 1, an inhibitor of IGF action, and mice with ablated IGF-I gene expression have brain growth retardation with impaired neuronal somatic and dendritic growth (19). The number of granule cells in the hippocampus, oligodendrocyte and neuron density within the olfactory bulbs, and total brain size are reduced in IGF-I knockout mice (19, 20). Furthermore, IGF-I gene deletion in humans is associated with mental retardation (21).

Ames dwarf mice are homozygous for a loss-of-function mutation at the Prop-1 locus ($Prop1^{df}$) (22, 23). This mutation impairs the development of the anterior pituitary resulting in dramatic depletion or absence of GH-, TSH-, and prolactin-producing cells in the adenohypophysis and primary deficiency of the corresponding hormones (23). Circulating IGF-I is undetectable in Ames dwarf mice because of the primary GH deficiency (16, 24). However, these mice have a significantly increased life span (22, 23) and maintain physiological function at youthful levels, including cognitive function (25). Recently, we found that old Ames dwarf mice have elevated levels of GH and IGF-I in the hippocampus, whereas the levels of the corresponding mRNAs are as high as in normal mice (26).

The aim of the present study was to investigate hippocampal GH and IGF-I expression in young adult dwarf mice and the association of the expression of these genes with neurogenesis in the DG of these mice.

Materials and Methods

Animals

Adult male Ames dwarf mice and age-matched normal male mice (12–13 wk old; n = 14 from each genotype) were used in the study. Normal mice were the siblings of the dwarfs. Animal protocols were reviewed and approved by the Southern Illinois University Animal Care and Use Committee. All animals had access to water and food *ad libitum*

First Published Online November 24, 2004

Abbreviations: BrdU, 5′-Bromo-2-deoxyuridine; Ct, threshold cycle number; DAB, diaminobenzidine; DG, dentate gyrus; FITC, fluorescein isothiocyanate; GAPDH, glyceraldehyde-3-phosphate dehydrogenase; GCL, granular cell layer; GFAP, glial fibrillary acidic protein; NeuN, neuronal nuclear antigen; SGZ, subgranular zone.

***Endocrinology* is published monthly by The Endocrine Society (http://www.endo-society.org), the foremost professional society serving the endocrine community.**

and were housed under a 12-h dark/12-h light cycle. Half of the mice were used for measuring gene expression (n = 7 from each group). The remaining animals were used for immunocytochemistry.

Antibodies

Primary antibodies and their final dilutions were as follows: polyclonal rat anti-bromodeoxyuridine (anti-BrdU), 1:500 (Accurate Chemical, Westbury, NY); monoclonal mouse anti-BrdU, 1:800 (Chemicon); polyclonal goat anti-GH IgG, 1:300 (Santa Cruz Biotechnology, Santa Cruz, CA); polyclonal rabbit anti-IGF-I IgG, 1:200 (Santa Cruz); mouse monoclonal anti-β-actin IgG, 1:2000 (Sigma Chemical Co., St. Louis, MO); mouse anti-neuronal nuclear antigen (anti-NeuN) IgG, 1:100 (Chemicon, Temecula, CA); and rabbit anti-glial fibrillary acidic protein (anti-GFAP) IgG, 1:300 (Dako, Carpinteria, CA). The following secondary antibodies from Jackson ImmunoResearch (Westgrove, PA) were used: fluorescein isothiocyanate (FITC)-conjugated donkey-mouse IgG, 1:500; FITC-conjugated donkey-rabbit IgG, 1:500; Rhodamine Red-X-conjugated donkey-goat IgG, 1:500; Rhodamine Red-X-conjugated donkey-mouse IgG, 1:500; Rhodamine Red-X-conjugated donkey-rat IgG, 1:500; or biotin-conjugated donkey-rat IgG, 1:500.

BrdU injections

Cell proliferation was measured by the incorporation of the thymidine analog 5′-bromo-2-deoxyuridine (BrdU), which is incorporated into the DNA of dividing cells in immunohistochemically detectable quantities during the S phase of cell division (27). Each animal was injected ip with BrdU (Sigma) (50 mg/kg at a concentration of 10 mg/ml in 0.9% NaCl) daily for seven consecutive days, and all animals were then killed 24 h after the last BrdU injection. The animals were anesthetized by ip injection of ketamine (50 mg/kg) and xylazine (10 mg/kg) and perfused with 0.9% NaCl followed by 4% paraformaldehyde.

Histology

After perfusion, brains were removed and postfixed overnight in 4% paraformaldehyde at 4 C. The brains were then equilibrated in 30% sucrose for an additional 24 h. Sections 40 μm thick were then prepared in the coronal plane using a freezing microtome.

Immunostaining

Diaminobenzidine (DAB) histochemical staining for BrdU was used for stereological quantification of labeled cells. Free-floating sections were treated with 0.6% H_2O_2 in PBS for 30 min to block endogenous peroxidase. For DNA denaturation, sections were incubated for 2 h in 50% formamide/2× standard saline citrate (0.3 M NaCl and 0.03 M sodium citrate) at 65 C, rinsed for 5 min in 2× standard saline citrate, incubated for 30 min in 2 N HCl at 37 C, and rinsed for 10 min in 0.1 M boric acid (pH 8.5). Several rinses in PBS were followed by incubation in PBS/0.1% Triton X-100/3% normal horse serum (PBS-Ths) for 30 min and incubation with mouse anti-BrdU antibody (Chemicon) in PBS-Ths overnight at +4 C. After being rinsed in PBS, sections were incubated for 1 h with secondary antimouse antibody (Vector Laboratories, Burlingame, CA). Tissues were washed in PBS and then incubated for 30 min in preassembled biotin-avidin-horseradish peroxidase complex according to the manufacturer's recommendations (ABC Elite, Vector). Sections were then washed and incubated in DAB solution for sufficient time to develop intense brown staining in BrdU-labeled nuclei. Rinsed sections were then mounted on uncoated Superfrost slides (Fisher Scientific, Santa Clara, CA), dried, and dehydrated through a graded alcohol series into xylenes and coverslipped with Permount mounting medium (Fisher).

Double-labeling immunofluorescence

Sections were treated for DNA denaturation as described above, followed by several rinses in PBS and incubation in PBS/0.1% Triton X-100/3% normal donkey serum for 30 min. For labeling of BrdU and cell-specific markers, sections were incubated with rat anti-BrdU (Accurate Chemical) and anti-NeuN (Chemicon) or anti-GFAP (Dako) at 4 C overnight followed by antirat Rhodamine Red-X IgG and antimouse or antirabbit FITC IgG for 2 h at room temperature and after thorough removal of primary antibodies. Sections were washed and wet mounted and then dried in the dark. Fluorescent mounting media was applied before placing coverslips onto the slides. For visualization and photography, specimens were observed under a confocal microscope.

Stereology/quantification of BrdU-labeled cells

Stereology was performed on tissues stained for BrdU using DAB histochemistry as described above. From all animals, every sixth section (240 μm apart) of the series was stained for BrdU with the peroxidase method. Positive cells were counted using a ×40 objective (Leica) throughout the rostrocaudal extent of the granule cell layer. The optical dissector method (28) was modified in that cells appearing sharp in the uppermost focal plane were not counted. Resulting numbers were multiplied by 6 to obtain the estimated total number of BrdU-positive cells per granule cell layer. BrdU-positive counts were limited to the hippocampal granular cell layer (GCL) and adjacent hilar subgranular zone (SGZ) margin using the fractionator probe (Stereo Investigator software, Microbrightfield, Williston, VT).

Fluorescently labeled tissue sections were evaluated using a Zeiss 510 confocal laser-scanning device (Carl Zeiss, Thornwood, NY) attached to a Zeiss-Axiovert microscope using LSM510 software. Appropriate gain and black-level settings were determined on control tissues stained with secondary antibodies alone. Upper and lower thresholds were set using the range indicator function to minimize saturation in positive cells. To assess the phenotype of BrdU-labeled cells, the number of BrdU- and/or NeuN-positive cells were scored within the dentate granule cell layer including the adjacent hilar margin or SGZ in the sections taken from the rostral, mid, and caudal hippocampus.

Real-time RT-PCR

Hippocampi (fresh) were dissected from the brain according to the procedures described by Glowinski *et al.* (29). Hippocampal tissue samples were stored at −70 C until the day of assay. The hippocampus was homogenized with RNA extraction buffer (TRIZOL reagent, Invitrogen Life Technologies, Inc., Carlsbad, CA) to yield total RNA following the manufacturer's instructions. Total RNA was reverse transcribed with poly-dT oligonucleotides and SuperScript II (Invitrogen Life Technologies), essentially under the manufacturer's recommended conditions. Briefly, 5 μl of the RNA was treated with DNase, and for the RT reaction, 3.6 μl DNase-treated RNA was combined with 2.5 μM oligo(deoxythymidine) primer and 500 μM of each dNTP. The mixture was then heated to 65 C for 5 min. Subsequently, 1× RT buffer [20 mM Tris-HCl (pH 8.4) and 50 mM KCl], 0.01 M dithiothreitol, 5 mM $MgCl_2$, and 2 U/μl RNaseOut ribonuclease inhibitor (Invitrogen Life Technologies) were added, and the mixture was heated to 42 C for 5 min. Fifty units of Superscript II reverse transcriptase (Invitrogen Life Technologies) were then added, and the reaction was performed at 42 C for 50 min, after which the reaction was stopped by heating at 70 C for 15 min.

Gene transcripts were quantified using a real-time PCR quantification system (SmartCycler, Cepheid, Sunnyvale, CA) and analyzed with SmartCycler software (version 1.2b). Primer sequences were designed using Primer Express Software (PerkinElmer Life Sciences, Boston, MA) and are presented in Table 1. After an initial denaturation step (95 C for 90 sec), amplification was performed over 40–45 cycles of denaturation (95 C for 10 sec), annealing (60 C for 5 sec), and elongation (72 C for 13 sec). Amplification was monitored by measuring the fluorometric intensity of SYBR Green I at the end of each elongation phase. In the PCR, reaction reagents were prepared as master mixes and then aliquotted into individual tubes to ensure uniform reaction conditions. Glyceraldehyde-3-phosphate dehydrogenase (GAPDH) expression was quantified to normalize the amount of cDNA in each sample. The specificity of the amplified product was monitored by its melting curve. Because the melting curve of a product is dependent upon its GC content, length, and sequence composition, specific amplification can be distinguished from nonspecific amplification by examining the melting curve (30, 31). A distinct single peak indicated that a single DNA sequence was amplified during PCR. In addition, end reaction products were visualized on ethidium bromide-stained 2% agarose gels. Appearance of a single band of the correct molecular size confirmed specificity of the PCR. Negative control experiments established that the signal for each am-

TABLE 1. Real-time RT-PCR primer sequence

Gene name	GenBank accession number	Primer orientation	Nucleotide sequence (from 5′ to 3′)	Size of the PCR amplicon (bp)
GAPDH	NM_008084	Forward	GAAGACACCAGTAGACTCCAC	207
		Reverse	AACGACCCCTTCATTGAC	
GH	NM_008117	Forward	AATGGCTACAGACTCTCGGA	127
		Reverse	CTCGGAGCACAGCATTAGAA	
IGF-1	NM_010512	Forward	CTGAGCTGGTGGATGCTCT	118
		Reverse	CACTCATCCACAATGCCTGT	

plicon was derived from cDNA and not from primer dimers. The change in threshold cycle number (ΔCt) was normalized to the GAPDH reference gene by subtracting ΔCt_{GAPDH} from ΔCt_{gene}. The effect of treatment (ΔΔCt) was calculated by subtracting ΔCt_{normal} from ΔCt_{dwarf}. Fold induction was determined by calculating $2^{-\Delta\Delta Ct}$. Data are reported as fold change of target cDNA in a dwarf sample relative to control. The identities of the PCR products were confirmed by sequencing through the Southern Illinois University sequencing facility.

Western blot analysis

Hippocampal proteins were obtained after RNA extraction. Total hippocampal proteins were determined by colorimetric method using BSA protein assay reagent (Pierce, Rockford, IL). Protein levels were quantified by Western blotting using antibodies specific for the respective proteins. In brief, homogenate proteins (40 μg per well) from mouse hippocampus were subjected to SDS-PAGE and then transferred to nitrocellulose membrane by electroblotting. For IGF-I antibody, the membrane was blocked in a buffer containing 50 mM Tris, 150 mM NaCl, 0.1% Tween 20, and 2.5% BSA (pH 7.5) for 2 h at 20 C. For other primary antibodies, membranes were blocked in a buffer containing 50 mM Tris, 150 mM NaCl, 0.1% Tween 20, and 5% milk (pH 7.5) for 2 h at 20 C. Subsequently, the membrane was incubated in appropriately diluted primary antibody (see reagents for different dilution) overnight at 4 C. After incubation and three washes, the membrane was probed with the specified horseradish peroxidase-linked second antibody for 2 h at 20 C. Antibodies were removed with stripping buffer (100 mM 2-mercaptoethanol/2% SDS/62.5 mM Tris-HCl, pH. 6.7) at 50 C for 30 min, followed by washing with PBS/Tween 20, and membranes were reprobed with β-actin antibody. Blots were processed using enhanced chemiluminescence (Amersham Pharmacia Biotech, Piscataway, NJ), and immunoreactive bands were viewed on an image analysis system consisting of a monochrome video camera (Dage MTI CCD 72; DAGE-MTI of MC, Inc., Michigan City, IN) connected to an Inter Focus Ltd. (MCID Imaging Research Inc., St. Catharines, Canada) image analysis system. The signals of the proteins were normalized to β-actin signals. Quantification of immunoblot signals was performed using GeneTools ImageQuant software (Syngene Inc., Frederick, MD).

IGF-I ELISA analysis

Concentrations of IGF-I in hippocampus homogenates were measured by ELISA using a commercial kit specific for mouse IGF-I (OCTEIA rat/mouse IGF-I ELISA kit, Immunodiagnostic Systems Inc., Fountain Hills, AZ) according to the manufacturer's protocol. Briefly, hippocampus homogenates (25 μl) in polystyrene tubes were pretreated for 10 min with a releasing reagent to denature IGF-binding protein. Samples were mixed with a diluent and were aliquotted in duplicate into microtiter strip wells coated with a polyclonal IGF-I antibody. A monoclonal IGF-I antibody labeled with horseradish peroxidase was added to the wells and incubated for 2 h at room temperature. After the incubation, wells were washed three times before addition of enzyme substrate. Samples were then incubated for 30 min. The resulting yellow acid dye at 450 nm with a reference filter of 620 nanometers was measured by a plate reader.

Statistical analyses

All data are presented as means ± SEM, and the statistical significance of differential findings between experimental groups and controls was determined by Student's *t* test or ANOVA for repeated measures using StatView version 4.5 (Abacus Concepts, Berkeley, CA). $P < 0.05$ was considered statistically significant.

Results

IGF-I mRNA and protein expression in the hippocampus of Ames dwarf mice

Real-time RT-PCR analyses indicate that expression of IGF-I mRNA in the hippocampus of Ames dwarf mice does not differ from the expression of this gene in the normal animals (Fig. 1). In contrast, an analysis of liver IGF-I mRNA levels found a ratio of 0.05, corresponding to a 20-fold reduction in liver IGF-I mRNA levels in Ames dwarf mice (data not shown). IGF-I values were normalized with GAPDH values. The identities of the PCR products were confirmed by sequencing. Western blot analysis of materials extracted from hippocampus revealed that IGF-I protein levels were significantly higher in Ames dwarf mice compared with the normal mice (Fig. 2). By densitometry, mean levels of IGF-I protein were 51 ± 2 U in dwarf hippocampal sample and 40 ± 3 U in the normal mice ($P < 0.03$). β-Actin expression was used as a control for protein loading. Furthermore, IGF-I levels in hippocampus tissue extracts were measured by ELISA. The estimated IGF-I concentration in the hippocampus of Ames dwarf mice was approximately 871.9 ± 40.1 pg/mg protein. The hippocampal IGF-I concentration in the normal mice was, for comparison, 714.8 ± 15.3 pg/mg protein (Fig. 3).

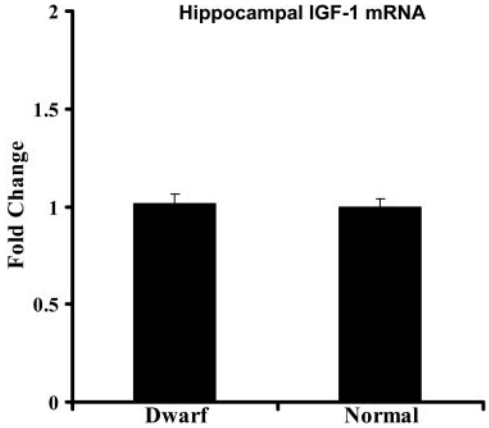

FIG. 1. IGF-1 mRNA expression in the hippocampus. Data are normalized with GAPDH values and are expressed as fold change of IGF-1 cDNA in dwarf mice sample relative to control.

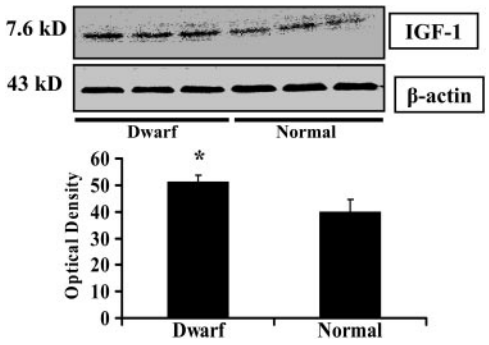

FIG. 2. Hippocampal IGF-1 protein expression. *Top*, Autoradiography of Western blot; *bottom*, densitometric analysis of Western blots. β-Actin signal was used to normalize the data. Each lane of the blots represents materials from a different normal or dwarf mouse. *, $P < 0.03$. A representative blot is shown.

GH mRNA and protein levels in the hippocampus of Ames dwarf mice

Real-time RT-PCR analyses indicate that GH mRNA in the hippocampus of Ames dwarf mice is reduced 5-fold compared with the expression in normal animals (Fig. 4). GH values were normalized with GAPDH values. The identities of the PCR products were also confirmed by sequencing. Consistent with mRNA expression, significant decreases of the GH protein level were observed in dwarf hippocampus compared with normal by Western blot (Fig. 5). Mean levels of GH protein were 58 ± 2 densitometry units in normal hippocampal sample and 37 ± 3 densitometry units in the dwarf mice ($P < 0.05$). β-Actin expression was used as a control for protein loading.

Evidence for increased neurogenesis in the DG of Ames dwarf mice

The number of newly generated cells in the adult DG was determined by monitoring the incorporation and subsequent immunohistochemical detection of BrdU within the nuclei of dividing cells (Fig. 6). Cells incorporating BrdU were found in the DG of all studied animals. BrdU-labeled cells in the GCL/SGZ appeared either isolated or in clusters (Fig. 6). BrdU-immunoreactive nuclei were located predominantly within the GCL or along the border between the GCL and the hilus. The nuclei were generally condensed and exhibited variable shapes. Quantitative analysis revealed that BrdU-immunoreactive cells were more abundant in the GCL/SGZ

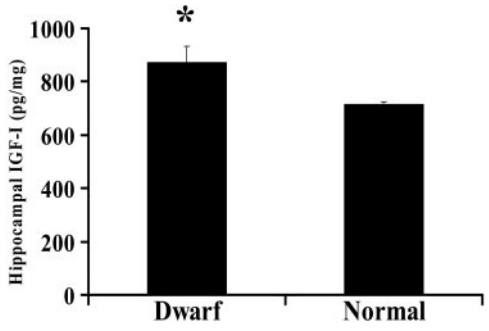

FIG. 3. Levels of IGF-I in hippocampus tissue homogenates were measured by ELISA from both dwarf and normal mice. *, $P < 0.05$.

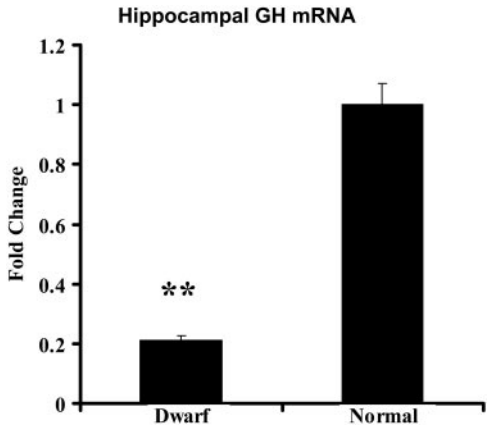

FIG. 4. GH mRNA expression in the hippocampus. Data are normalized with GAPDH values and are expressed as fold change of GH cDNA in dwarf mice sample relative to control. **, $P < 0.001$.

of Ames dwarf mice compared with the normal mice. To determine the phenotypes of the BrdU-labeled cells, we performed double-labeling confocal immunohistochemical analysis of brain sections using an antibody against the mature astrocyte marker GFAP or an antibody against the mature neuron-specific protein NeuN and an antibody against BrdU (Fig. 7). Double-labeling studies indicated that 21% of BrdU-labeled cells in the DG area were of a neuronal phenotype (NeuN positive), 4.4% were astrocytes (GFAP positive), and the rest were undefined (NeuN or GFAP negative). Ongoing studies of double-labeling BrdU with early neuronal marker (doublecortin or the β-III-tubulin protein TuJ1) show that the immature neurons are approximately 75% totally BrdU-labeled cells (data not shown). Those BrdU- and NeuN-positive cells are also significantly increased in dwarf mice compared with normal mice (Fig. 8). Using a series of Z-step section scans, we were able to confirm that BrdU-positive cells located in the GCL of the DG showed a neuronal phenotype. BrdU-labeled cells were seen not only in the DG but also in several other brain areas including hippocampal regions CA1 and CA3 and cerebral cortex, but these cells were not immunoreactive with the NeuN or GFAP antibodies.

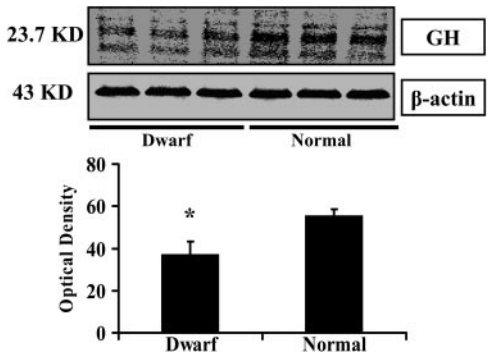

FIG. 5. Hippocampal GH protein levels. *Top*, Autoradiography of Western blot; *bottom*, densitometric analysis of western blots. β-Actin signal was used to normalize the data. Each lane of the blots represents materials from a different normal or dwarf mouse. *, $P < 0.05$. A representative blot is shown.

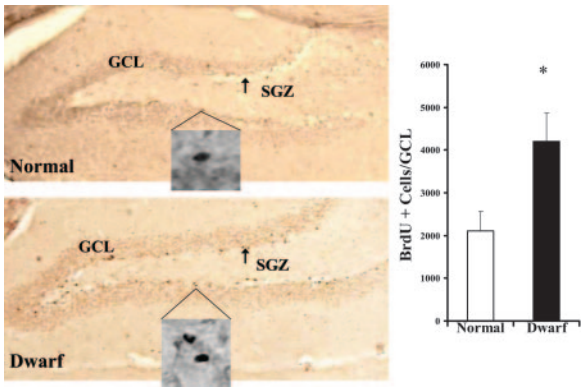

FIG. 6. Neural progenitor cells are increased in the hippocampus of Ames dwarf mice. Representative micrograph showing BrdU-immunopositive cells in the SGZ of the DG in normal mice and Ames dwarf mice. *Scale bar*, 40 μm. *Right*, Results of quantification of BrdU-immunopositive cells in the GCL of the DG of dwarf mice and normal mice. *, $P < 0.005$.

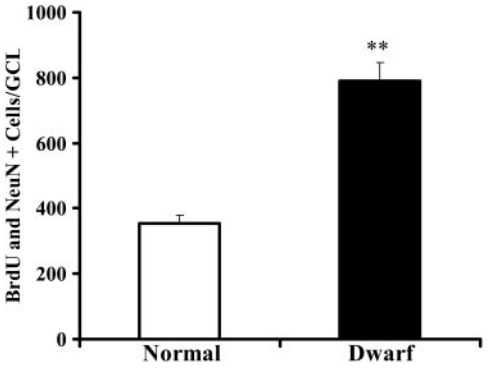

FIG. 8. Results of quantification of BrdU/NeuN double-positive cells in the GCL of the DG of dwarf mice and normal mice. **, $P < 0.005$.

Discussion

In summary, dwarf animals showed an overall increase in the number of dividing cells within the SGZ as well as a striking increase in both the total number of newly generated cells (BrdU positive) and newborn neurons (NeuN and BrdU positive) within this population of cells. Consistent with the previous observation in old animals, hippocampal-derived IGF-I was also up-regulated in young adult Ames dwarf mice. These results point out that locally produced IGF-I may have induced an increase in overall proliferative activity of uncommitted progenitor cells and favored the accumulation of neuron-committed progenitor cells. Increased neurogenesis might contribute to the amelioration of cognitive deficits during aging in these long-lived animals. Recent studies show that IGF-I may play an important role in neurogenesis in the adult mammalian brain (32). Exogenous administration of IGF-I is also known to stimulate neurogenesis (33, 34). Furthermore, blockade of circulating IGF-I by injections of a neutralizing antibody suppresses basal neurogenesis (34). Blockade of IGF-I has also been shown to prevent exercise-induced neurogenesis, demonstrating IGF-I as a necessary component of physical activity-induced neurogenesis (33). Given the previous evidence that circulating IGF-I is undetectable in Ames dwarf mice (24), the IGF-I immunoreactivity detected by Western blot in the hippocampus seems unlikely to be derived from peripheral circulation and transport across the blood-brain barrier. Thus, IGF-I might be produced locally in the hippocampus and might also act directly on the neuronal progenitor cells in the DG. Enhanced neurogenesis in dwarf mice that we reported here has certain features that merit consideration. Because we measured neurogenesis only by BrdU and NeuN/GFAP labeling, our current data do not fully address subsequent events of neurogenesis, such as neuronal migration, further developmental maturation, and long-term survival. In addition, with the current BrdU injection protocol, the number of newly generated cells or neurons represents a combination of the proliferation rate, the differentiation rate, and net cell survival/apoptosis. It will be important to investigate the role of apoptosis in the regulation of adult neurogenesis in dwarf mice. Future studies will focus on these issues.

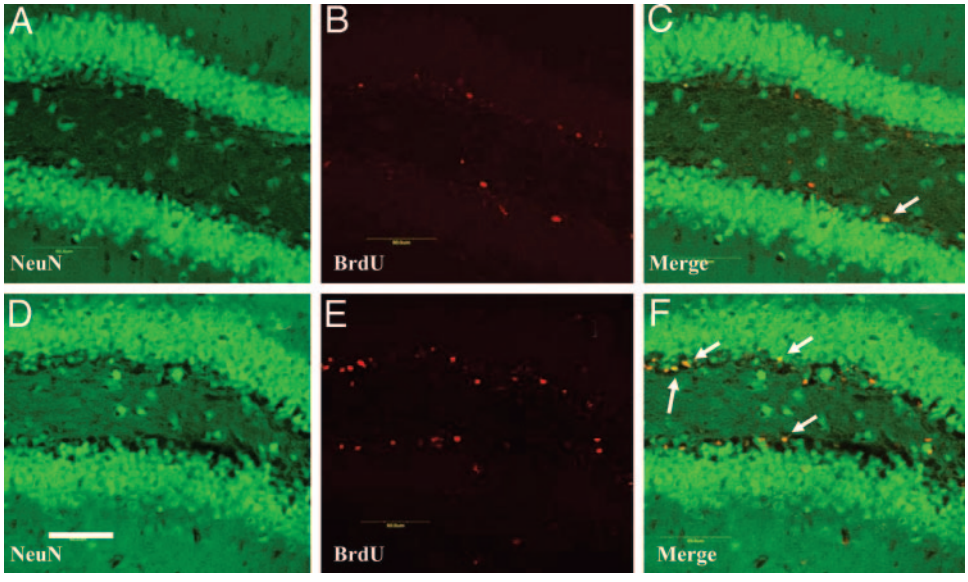

FIG. 7. Characterization of newly generated cells in SGZ. Confocal images of newborn cells in the hippocampus of normal mice (A–C) and Ames dwarf mice (D–F). Cells immunofluorescently labeled for NeuN (neuronal phenotype marker) were green (A and D) and for BrdU were red (B and E). Merged images (C and F) show both BrdU/NeuN-positive cells. *Scale bar*, 50 μm.

IGF-I, glia cells, and neurogenic microenvironment

Neural progenitor cell expansion and differentiation are regulated *in vivo* by environmental factors encountered in the neurogenic niche (35). The generation of new neurons within the hippocampus is mediated by proliferating neural stem cells and instructed by local signaling to produce neurons only in specific areas (1). Alterations in the microenvironment of the neural stem cell may allow ectopic neurogenesis to occur (36) or even block essential neurogenesis (37). For example, cranial irradiation ablates mouse hippocampal neurogenesis by damaging the neurogenic microenvironment (38). Moreover, neural stem cells *in vivo* are likely to be influenced by a convergence of signals from many neighboring cell types. Astrocytes, for instance, enhance the proliferative and neurogenic properties of neural stem cells by a factor of 2 and 6, respectively (39). It has been shown that microglia and astrocytes in the hippocampus induced neurogenesis from neural stem cells (39, 40). Glial cells can synthesize and release significant amounts of IGF-I *in vivo* and *in vitro* (41–43). Preliminary results in our laboratory showed that distinct glial cell populations in the hippocampus of dwarf mice exhibited selective enrichment for GH or IGF-I expression (data not shown). Therefore, glial cells are uniquely poised to act as sensors and regulators in the stem cell niche probably by the secretion of instructive signaling factors including IGF-I in the hippocampal neurogenic microenvironment.

Locally produced IGF-I and GH in the hippocampus

Of various regulators of IGF-I production, GH is probably the most important, capable of regulating both endocrine (liver-derived) and local levels (44). However, in the present study, GH mRNA and protein were lower in dwarf hippocampus compared with normal, whereas IGF-I mRNA levels were as high as normal and IGF-I protein was upregulated in dwarf animals. Thus, changes in IGF-I protein levels in the hippocampus of dwarf *vs.* normal mice did not correspond to alterations in hippocampal levels of GH in these animals. Furthermore, our ongoing studies in GH receptor and binding protein knockout mice suggest that substantial IGF-I expression in the brain can be detected in the absence of GH signaling. Interestingly, similar findings were previously reported in the independently produced GH receptor knockout mice from Efstratiadis' group (45). Taken together, this evidence suggests that hippocampal or brain IGF-I might be GH independent.

GH is synthesized and stored by somatotroph cells within the anterior pituitary gland (44). Our initial work showed that both GH mRNA and protein could be detected in the hippocampus of old Ames dwarf mice, which are characterized by absence of pituitary GH because of the loss-of-function mutation at the Prop 1 locus and the resulting failure of somatotroph differentiation. Current data further support the existence of extrapituitary GH in the murine brain (26). Interestingly, hippocampal GH expression is suppressed in young dwarf mice but not in old dwarf animals when compared with the normal control mice. However, why this occurs and the mechanisms responsible for the change remain uncertain.

The current study reports the novel finding that the locally/hippocampal-synthesized IGF-I might be an important regulator in hippocampal neurogenesis in the DG of Ames dwarf mice and suggests that local hormone expression seems to be able to maintain central nervous system function independently of regulation by the hypothalamic-pituitary axis. However, we do not provide a proof of causality. Additional experiments will be needed to elucidate this issue, and additional studies will also be needed to identify or eliminate the possible role of TSH and prolactin deficiency in the hippocampal neurogenesis of dwarf mice.

Acknowledgments

We thank Drs. Richard A. Miller and Luis M. Garcia-Segura for critique of the manuscript. We also thank members of Dr. Bartke's laboratory for helpful discussions on the study.

Received August 23, 2004. Accepted November 15, 2004.

Address all correspondence and requests for reprints to: Dr. Andrzej Bartke, Southern Illinois University, School of Medicine, Department of Internal Medicine-Geriatrics Research, Room 4389, 801 North Rutledge, Springfield, Illinois 62794-9628. E-mail: abartke@siumed.edu.

This work was supported by National Institutes of Health Grant AG019899 and the Ellison Medical Foundation Grant (to A.B.), by Glenn Foundation/AFAR Scholarships (to L.S.), and by Southern Illinois University Geriatrics Medicine and Research Initiative.

References

1. **Gage FH** 2000 Mammalian neural stem cells. Science 287:1433–1438
2. **Cameron HA, Gould E** 1994 Adult neurogenesis is regulated by adrenal steroids in the dentate gyrus. Neuroscience 61:203–209
3. **Eriksson PS, Perfilieva E, Bjork-Eriksson T, Alborn AM, Nordborg C, Peterson DA, Gage FH** 1998 Neurogenesis in the adult human hippocampus. Nat Med 4:1313–1317
4. **Gould E, Reeves AJ, Fallah M, Tanapat P, Gross CG, Fuchs E** 1999 Hippocampal neurogenesis in adult Old World primates. Proc Natl Acad Sci USA 96:5263–5267
5. **Suhonen JO, Peterson DA, Ray J, Gage FH** 1996 Differentiation of adult hippocampus-derived progenitors into olfactory neurons in vivo. Nature 383: 624–627
6. **Shors TJ, Miesegaes G, Beylin A, Zhao M, Rydel T, Gould E** 2001 Neurogenesis in the adult is involved in the formation of trace memories. Nature 410:372–376
7. **Macklis JD** 2001 Neurobiology: new memories from new neurons. Nature 410:314–315, 317
8. **Hodges H, Veizovic T, Bray N, French SJ, Rashid TP, Chadwick A, Patel S, Gray JA** 2000 Conditionally immortal neuroepithelial stem cell grafts reverse age-associated memory impairments in rats. Neuroscience 101:945–955
9. **Qu T, Brannen CL, Kim HM, Sugaya K** 2001 Human neural stem cells improve cognitive function of aged brain. Neuroreport 12:1127–1132
10. **Lee J, Duan W, Mattson MP** 2002 Evidence that brain-derived neurotrophic factor is required for basal neurogenesis and mediates, in part, the enhancement of neurogenesis by dietary restriction in the hippocampus of adult mice. J Neurochem 82:1367–1375
11. **Gould E, Tanapat P** 1997 Lesion-induced proliferation of neuronal progenitors in the dentate gyrus of the adult rat. Neuroscience 80:427–436
12. **Kempermann G, Kuhn HG, Gage FH** 1997 More hippocampal neurons in adult mice living in an enriched environment. Nature 386:493–495
13. **van Praag H, Kempermann G, Gage FH** 1999 Running increases cell proliferation and neurogenesis in the adult mouse dentate gyrus. Nat Neurosci 2:266–270
14. **Bondolfi L, Ermini F, Long JM, Ingram DK, Jucker M** 2004 Impact of age and caloric restriction on neurogenesis in the dentate gyrus of C57BL/6 mice. Neurobiol Aging 25:333–340
15. **D'Ercole AJ, Ye P, Calikoglu AS, Gutierrez-Ospina G** 1996 The role of the insulin-like growth factors in the central nervous system. Mol Neurobiol 13: 227–255
16. **Bartke A, Chandrashekar V, Dominici F, Turyn D, Kinney B, Steger R, Kopchick JJ** 2003 Insulin-like growth factor 1 (IGF-1) and aging: controversies and new insights. Biogerontology 4:1–8
17. **Carson MJ, Behringer RR, Brinster RL, McMorris FA** 1993 Insulin-like growth factor I increases brain growth and central nervous system myelination in transgenic mice. Neuron 10:729–740

18. **Lee KH, Calikoglu AS, Ye P, D'Ercole AJ** 1999 Insulin-like growth factor-I (IGF-I) ameliorates and IGF binding protein-1 (IGFBP-1) exacerbates the effects of undernutrition on brain growth during early postnatal life: studies in IGF-I and IGFBP-1 transgenic mice. Pediatr Res 45:331–336
19. **Cheng CM, Mervis RF, Niu SL, Salem Jr N, Witters LA, Tseng V, Reinhardt R, Bondy CA** 2003 Insulin-like growth factor 1 is essential for normal dendritic growth. J Neurosci Res 73:1–9
20. **Ye P, Li L, Richards RG, DiAugustine RP, D'Ercole AJ** 2002 Myelination is altered in insulin-like growth factor-I null mutant mice. J Neurosci 22:6041–6051
21. **Woods KA, Camacho-Hubner C, Savage MO, Clark AJ** 1996 Intrauterine growth retardation and postnatal growth failure associated with deletion of the insulin-like growth factor I gene. N Engl J Med 335:1363–1367
22. **Brown-Borg HM, Borg KE, Meliska CJ, Bartke A** 1996 Dwarf mice and the ageing process. Nature 384:33
23. **Bartke A, Brown-Borg H, Mattison J, Kinney B, Hauck S, Wright C** 2001 Prolonged longevity of hypopituitary dwarf mice. Exp Gerontol 36:21–28
24. **Chandrashekar V, Bartke A** 1993 Induction of endogenous insulin-like growth factor-I secretion alters the hypothalamic-pituitary-testicular function in growth hormone-deficient adult dwarf mice. Biol Reprod 48:544–551
25. **Kinney BA, Meliska CJ, Steger RW, Bartke A** 2001 Evidence that Ames dwarf mice age differently from their normal siblings in behavioral and learning and memory parameters. Horm Behav 39:277–284
26. **Sun LY, Al-Regaiey K, Masternak MM, Wang J, Bartke A** 11 November 2004 Local expression of growth hormone and insulin-like growth factor 1 in the hippocampus of long-lived mice. Neurobiol Aging 10.1016/jneurobiolaging.2004.07.010
27. **Altman J, Das GD** 1965 Autoradiographic and histological evidence of postnatal hippocampal neurogenesis in rats. J Comp Neurol 124:319–335
28. **Williams RW, Rakic P** 1988 Three-dimensional counting: an accurate and direct method to estimate numbers of cells in sectioned material. J Comp Neurol 278:344–352
29. **Glowinski J, Iversen LL** 1966 Regional studies of catecholamines in the rat brain. I. The disposition of [^{3}H]norepinephrine, [^{3}H]dopamine and [^{3}H]dopa in various regions of the brain. J Neurochem 13:655–669
30. **Dhar AK, Roux MM, Klimpel KR** 2002 Quantitative assay for measuring the Taura syndrome virus and yellow head virus load in shrimp by real-time RT-PCR using SYBR Green chemistry. J Virol Methods 104:69–82
31. **Ririe KM, Rasmussen RP, Wittwer CT** 1997 Product differentiation by analysis of DNA melting curves during the polymerase chain reaction. Anal Biochem 245:154–160
32. **Anderson MF, Aberg MA, Nilsson M, Eriksson PS** 2002 Insulin-like growth factor-I and neurogenesis in the adult mammalian brain. Brain Res Dev Brain Res 134:115–122
33. **Trejo JL, Carro E, Torres-Aleman I** 2001 Circulating insulin-like growth factor I mediates exercise-induced increases in the number of new neurons in the adult hippocampus. J Neurosci 21:1628–1634
34. **Aberg MA, Aberg ND, Hedbacker H, Oscarsson J, Eriksson PS** 2000 Peripheral infusion of IGF-I selectively induces neurogenesis in the adult rat hippocampus. J Neurosci 20:2896–2903
35. **Doetsch F** 2003 A niche for adult neural stem cells. Curr Opin Genet Dev 13:543–550
36. **Magavi SS, Leavitt BR, Macklis JD** 2000 Induction of neurogenesis in the neocortex of adult mice. Nature 405:951–955
37. **Monje ML, Toda H, Palmer TD** 2003 Inflammatory blockade restores adult hippocampal neurogenesis. Science 302:1760–1765
38. **Monje ML, Mizumatsu S, Fike JR, Palmer TD** 2002 Irradiation induces neural precursor-cell dysfunction. Nat Med 8:955–962
39. **Song H, Stevens CF, Gage FH** 2002 Astroglia induce neurogenesis from adult neural stem cells. Nature 417:39–44
40. **Aarum J, Sandberg K, Haeberlein SL, Persson MA** 2003 Migration and differentiation of neural precursor cells can be directed by microglia. Proc Natl Acad Sci USA 100:15983–15988
41. **Fernandez-Galaz MC, Morschl E, Chowen JA, Torres-Aleman I, Naftolin F, Garcia-Segura LM** 1997 Role of astroglia and insulin-like growth factor-I in gonadal hormone-dependent synaptic plasticity. Brain Res Bull 44:525–531
42. **Bondy C, Werner H, Roberts Jr CT, LeRoith D** 1992 Cellular pattern of type-I insulin-like growth factor receptor gene expression during maturation of the rat brain: comparison with insulin-like growth factors I and II. Neuroscience 46:909–923
43. **Du Y, Dreyfus CF** 2002 Oligodendrocytes as providers of growth factors. J Neurosci Res 68:647–654
44. **Kopchick JJ, Andry JM** 2000 Growth hormone (GH), GH receptor, and signal transduction. Mol Genet Metab 71:293–314
45. **Lupu F, Terwilliger JD, Lee K, Segre GV, Efstratiadis A** 2001 Roles of growth hormone and insulin-like growth factor 1 in mouse postnatal growth. Dev Biol 229:141–162

***Endocrinology* is published monthly by The Endocrine Society (http://www.endo-society.org), the foremost professional society serving the endocrine community.**